

Electronic Supplementary Information

**Surface coverage control for dramatic enhancement of thermal CO
oxidation by precise potential tuning of metal supported catalysts**

Xingyu Qi,^a Tatsuya Shinagawa,^a Xiaofei Lu,^a Yuhki Yui,^b Masaya Ibe^b and Kazuhiro Takanabe*^a

^a *Department of Chemical System Engineering, School of Engineering, The University of Tokyo, 7-3-1 Hongo, Bunkyo-ku, Tokyo, Japan.*

^b *Advanced Material Engineering Division, Higashifuji Technical Center, Toyota Motor Corporation, 1200 Mishuku, Susono, Shizuoka, Japan.*

Corresponding author: Prof. Kazuhiro Takanabe, Email: takanabe@chemsys.t.u-tokyo.ac.jp

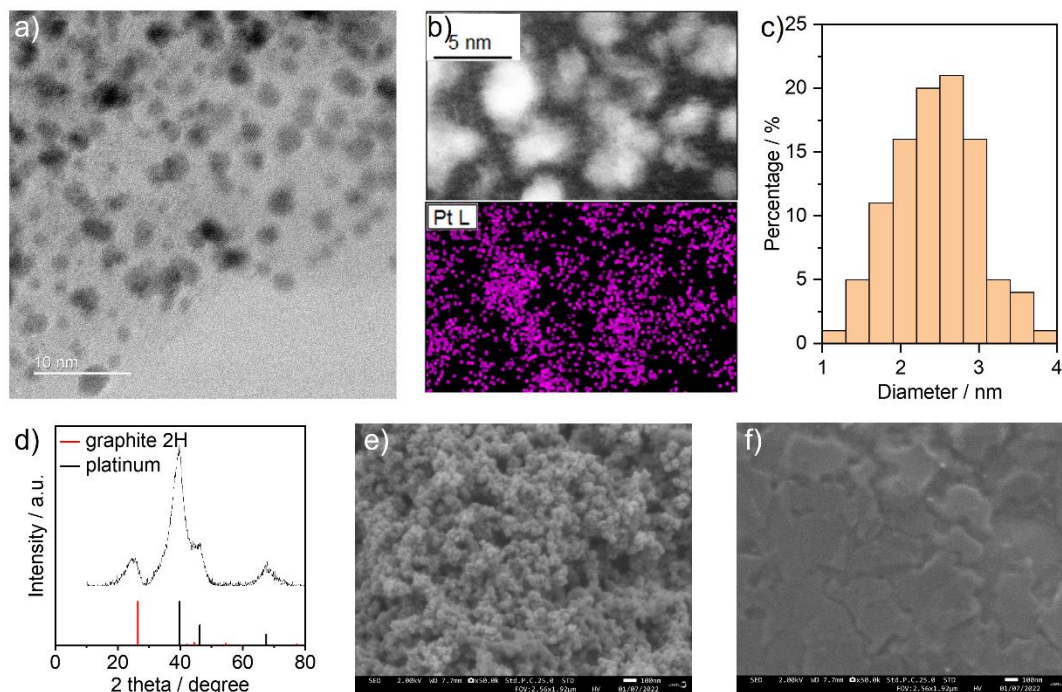


Fig. S1. **a)** TEM image, **b)** EDX-mapping image, **c)** distribution of particle sizes, **d)** XRD characterization of pristine Pt/C catalyst and SEM images of **e)** pristine Pt/C layer on CP substrate and **f)** pristine CP substrate.

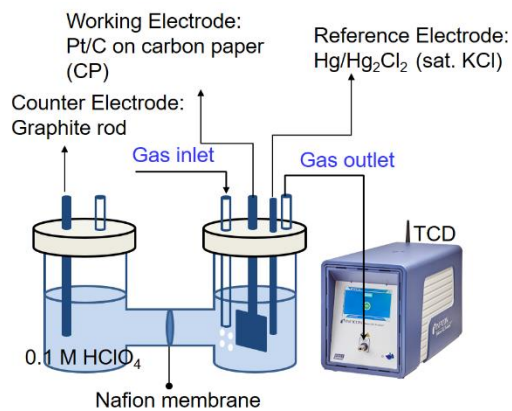


Fig. S2. Schematic representation of the two-compartment cell (H-cell) used for catalytic measurement.

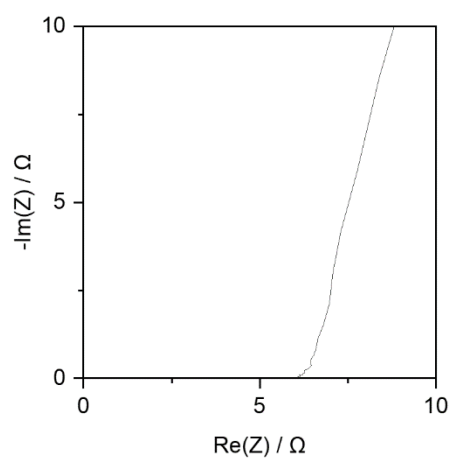


Fig. S3. PEIS profile for resistance determination. Conditions: WE: 3 mg Pt/C on $2 \times 2 \text{ cm}^2$ CP; potential: 0.70 V vs. RHE; initial frequency: 200 kHz; final frequency: 100 mHz; gas flow rate: 20 ml min^{-1} ; pressure: 101 kPa; $p(\text{CO})$: 25 kPa; $p(\text{O}_2)$: 10 kPa; balance: Ar; RE: Hg/Hg₂Cl₂ (sat. KCl); CE: graphite rod; 295 K; stirring rate: 750 rpm; 0.1 M HClO₄.

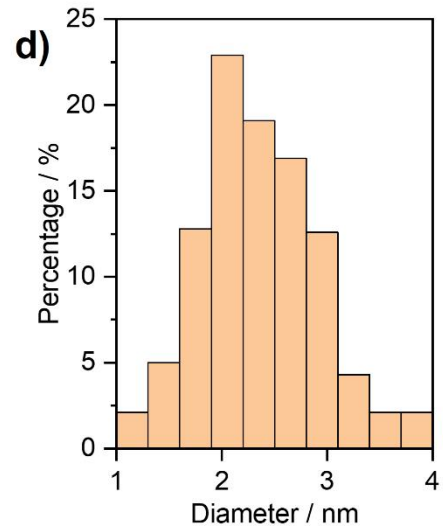
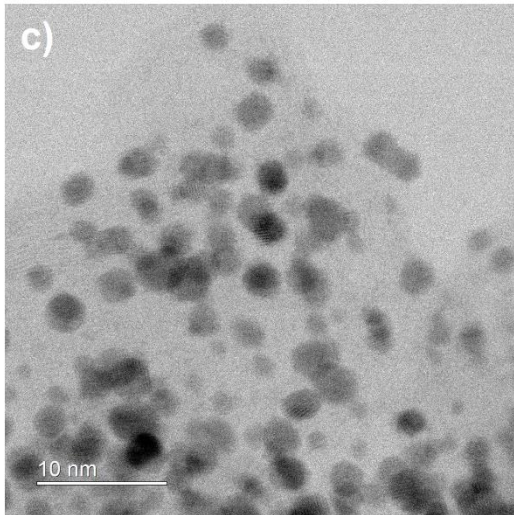
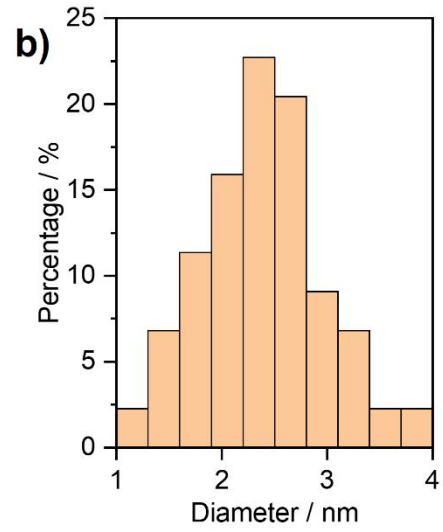
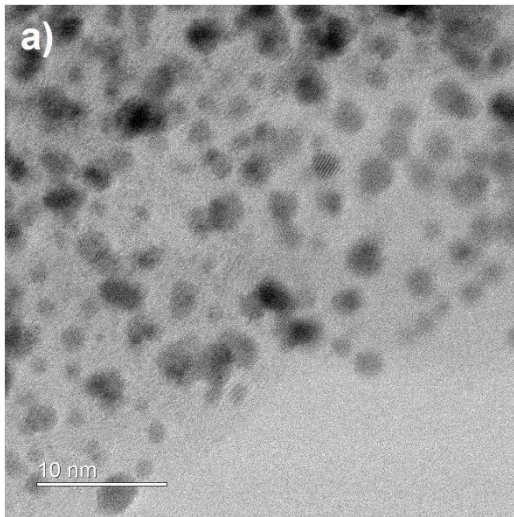


Fig. S4. a) TEM image and b) distribution of particle sizes of Pt/C catalyst after OCP-shift measurement. c) TEM image and d) distribution of particle sizes of Pt/C catalyst after 4-h reaction under 25 kPa CO and 10 kPa O₂ with 0.70 V vs. RHE applied.

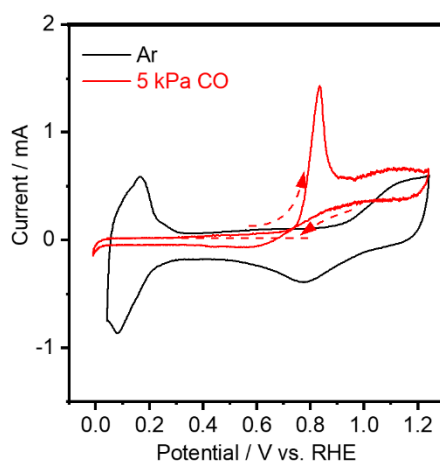


Fig. S5. Cyclic voltammetry (CV) characterization of Pt/C catalyst under pure Ar or diluted CO. Conditions: WE: 0.75 mg Pt/C on $1 \times 1 \text{ cm}^2$ CP; gas flow rate: 20 ml min^{-1} ; pressure: 101 kPa; Scan rate: 2 mV s^{-1} ; RE: Hg/Hg₂Cl₂ (sat. KCl); CE: graphite rod; 295 K; stirring rate: 750 rpm; 0.1 M HClO₄.

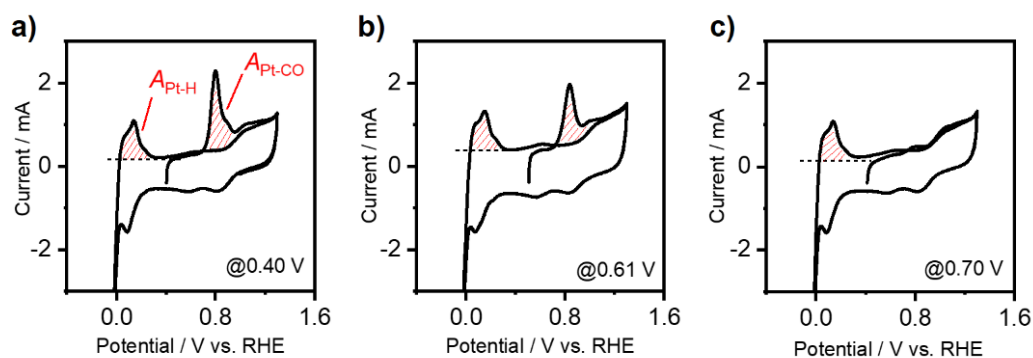


Fig. S6. CV profiles used for CO* coverage (θ_{CO}) calculation at **a)** 0.40 V, **b)** 0.61 V, and **c)** 0.70 V vs. RHE. WE: 0.75 mg Pt/C on $1 \times 1 \text{ cm}^2$ CP; gas flow rate: 20 ml min^{-1} ; pressure: 101 kPa; Scan rate: 1 mV s^{-1} ; RE: Hg/Hg₂Cl₂ (sat. KCl); CE: graphite rod; 295 K; stirring rate: 750 rpm; 0.1 M HClO₄.

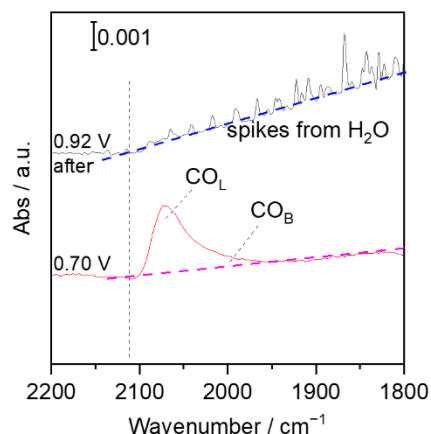


Fig. S7. Infrared spectra at 0.70 V (red) and 0.92 V (black) vs. RHE under 25 kPa CO and 10 kPa O₂. The baseline for the integral of CO* band was determined based on the baseline appearing in the case of 0.92 V.

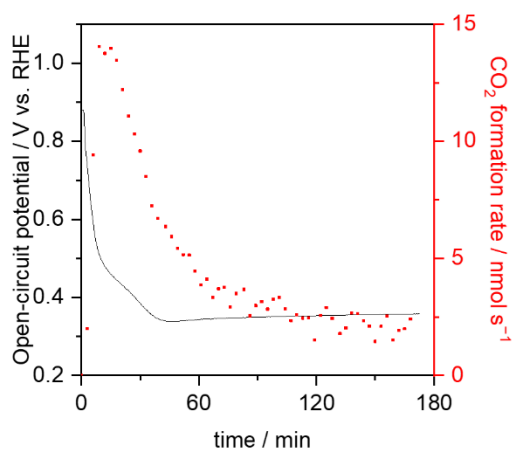


Fig. S8. Time evolution of open-circuit potential of Pt/C catalyst during CO oxidation and corresponding reaction rate. Conditions: WE: 3 mg Pt/C on 2×2 cm² CP; gas flow rate: 20 ml min⁻¹; pressure: 101 kPa; $p(\text{CO})$: 25 kPa; $p(\text{O}_2)$: 10 kPa; RE: Hg/Hg₂Cl₂ (sat. KCl); CE: graphite rod; stirring rate: 750 rpm; 295 K; 0.1 M HClO₄.

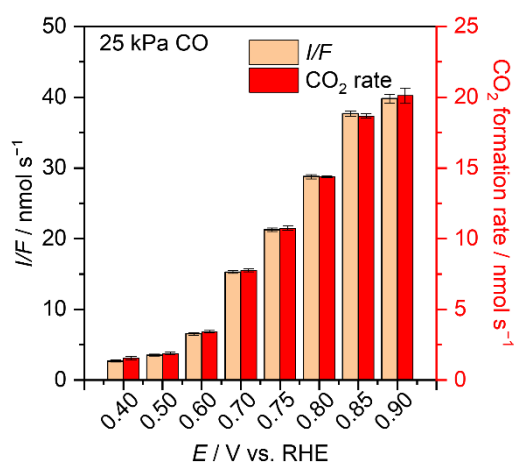


Fig. S9. Comparison of electric current and corresponding CO₂ formation rate in unit of nmol s⁻¹ at varied potentials, showing a ratio of ~2 and indicating a FE of ~100% for electrochemical CO oxidation under the given condition. Conditions: WE: 3 mg Pt/C on 2×2 cm² CP; gas flow rate: 20 ml min⁻¹; pressure: 101 kPa; *p*(CO): 25 kPa; balance: Ar; RE: Hg/Hg₂Cl₂ (sat. KCl); CE: graphite rod; 295 K; stirring rate: 750 rpm; 0.1 M HClO₄.

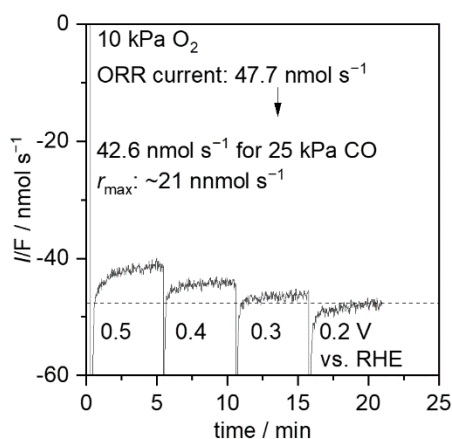


Fig. S10. Measurement of diffusion-limited ORR current for the estimation of diffusion-limited CO oxidation rate. Conditions: WE: 3 mg Pt/C on 2×2 cm² CP; gas flow rate: 20 ml min⁻¹; pressure: 101 kPa; *p*(O₂): 10 kPa; balance: Ar; RE: Hg/Hg₂Cl₂ (sat. KCl); CE: graphite rod; 295 K; stirring rate: 750 rpm; 0.1 M HClO₄.

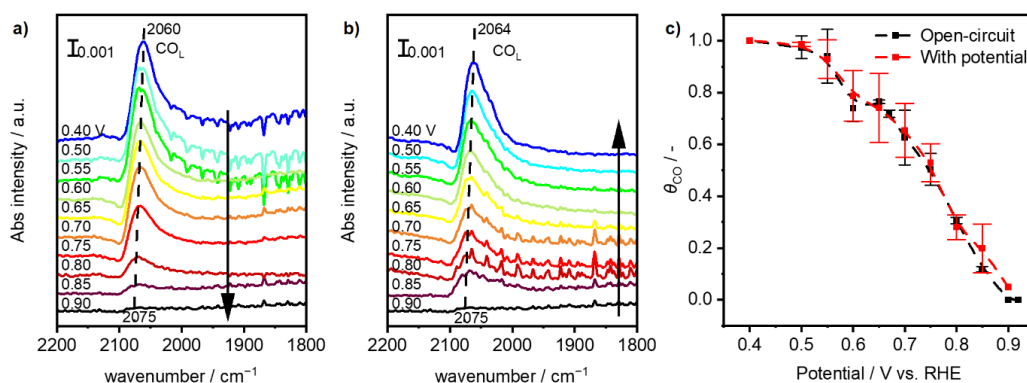


Fig. S11. The evolution of infrared spectra with external potential **a)** changing from 0.40 V to 0.90 V vs. RHE and **b)** changing from 0.90 V back to 0.40 V vs. RHE. **c)** Calculated θ_{CO} as a function of external potential based on ATR-IRAS. Conditions: WE: Pt/C on IRE; gas flow rate: 20 ml min⁻¹; pressure: 101 kPa; balance: Ar; RE: Hg/Hg₂Cl₂ (sat. KCl); CE: Pt wire; 0.1 M HClO₄; 295 K.

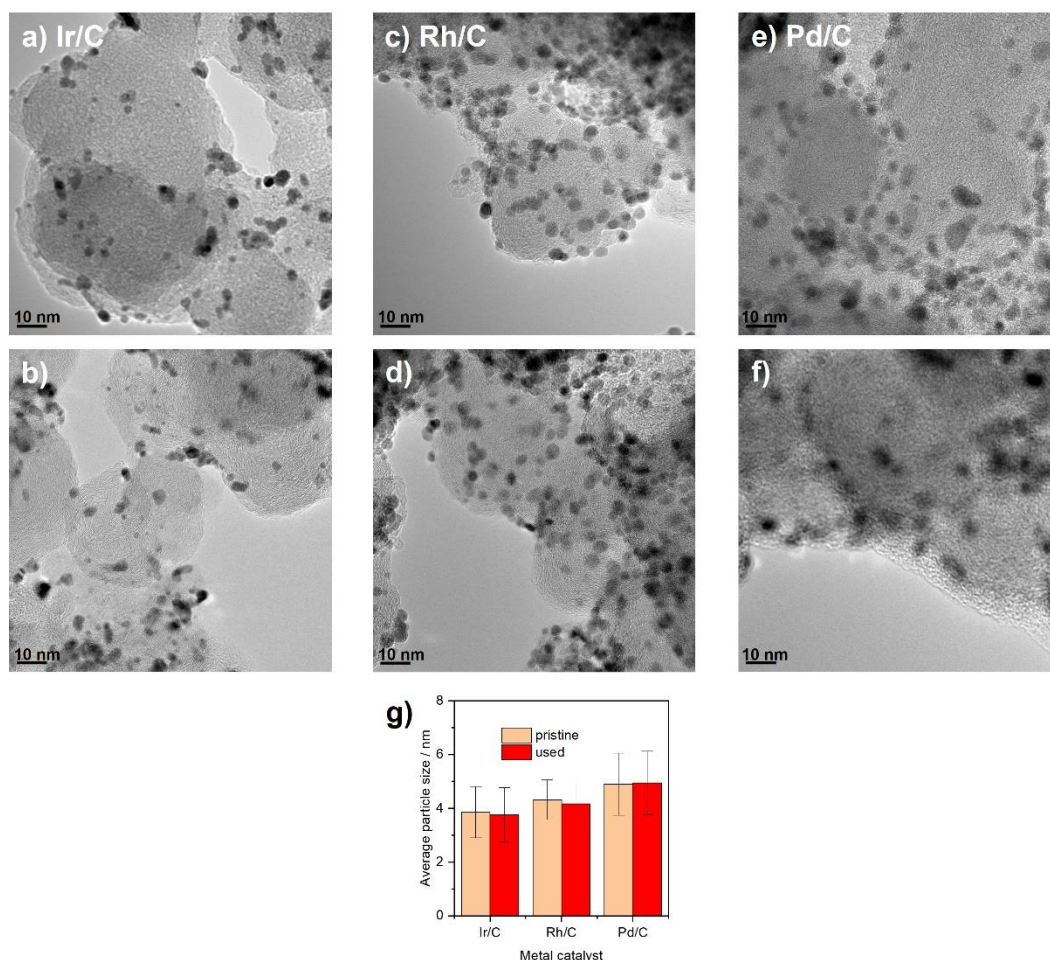


Fig. S12. TEM images of **a)** pristine Ir/C, **b)** used Ir/C, **c)** pristine Rh/C, **d)** used Rh/C, **e)** pristine Pd/C and **f)** used Pd/C, and **g)** statistical comparison of particle sizes of pristine and used catalysts. Reaction potential: 0.75 V vs. RHE for Ir/C, 0.70 V for Rh/C and 0.90 V for Pd/C (potentials for the best FE).

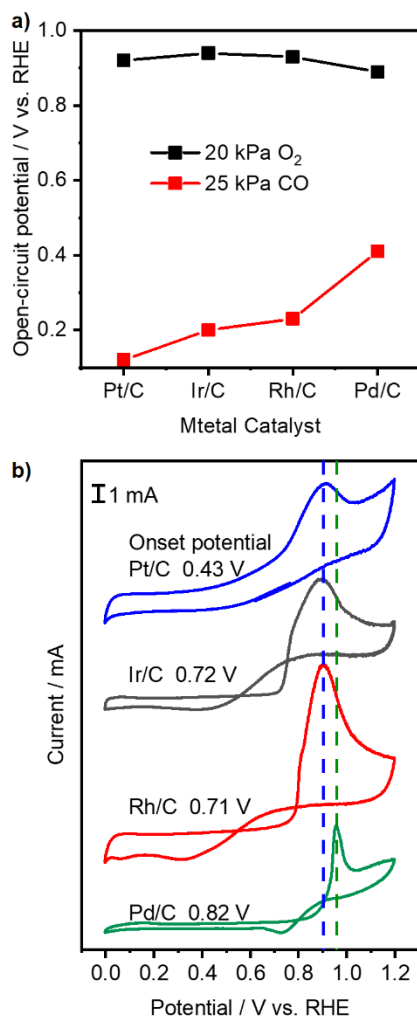


Fig. S13. a) OCP values of metal catalysts under 20 kPa O₂ or 25 kPa CO. **b)** CV profiles of metal catalysts under 25 kPa CO. Conditions: WE: 3 mg metal/C on 2×2 cm² CP; gas flow rate: 20 ml min⁻¹; pressure: 101 kPa; balance: Ar; RE: Hg/Hg₂Cl₂ (sat. KCl); CE: graphite rod; stirring rate: 750 rpm; scan rate: 2 mV s⁻¹; 295 K; 0.1 M HClO₄.

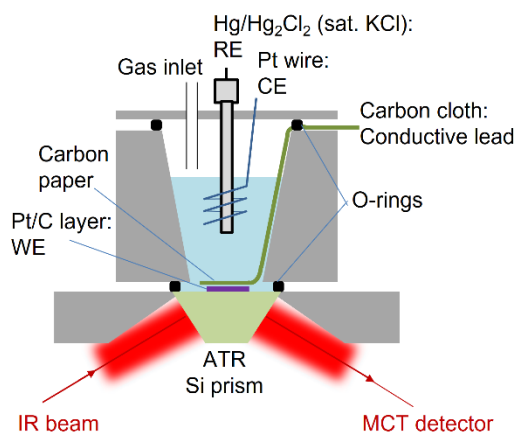


Fig. S14. Schematic presentation of the electrochemical cell for in situ attenuated total reflection-infrared absorption spectroscopy (ATR-IRAS) measurement.